



Construction of a Biocompatible and Antioxidant Multilayer Coating by Layer-by-Layer Assembly of κ -Carrageenan and Quercetin Nanoparticles

Marthyna P. Souza^{1,2,3} · Antônio F. M. Vaz⁴ · Thacianna B. Costa² · Miguel A. Cerqueira^{3,5} · Célia M. M. B. De Castro² · Antônio A. Vicente³ · Maria G. Carneiro-da-Cunha^{1,2} 

Received: 27 September 2017 / Accepted: 2 February 2018
© Springer Science+Business Media, LLC, part of Springer Nature 2018

Abstract

The present work aimed at the construction and characterization of a multilayer coating based on κ -carrageenan and quercetin-loaded lecithin/chitosan nanoparticles (Np) by the layer-by-layer technique and the evaluation of its antioxidant capacity and potential cytotoxicity *in vitro*. The multilayered coating was successfully self-assembled, as confirmed by UV-Vis spectroscopy, contact angle, atomic force microscopy (AFM), and scanning electron microscopy (SEM). Multilayered coatings showed to have antioxidant capacity, with a DPPH• radical scavenging activity of $31.32 \pm 3.13\%$ and a result of the FRAP assay of $799.41 \pm 95.39 \mu\text{M}$ of ferrous ion (Fe^{2+}) equivalent. These coatings were also shown to be devoid of cell toxicity, as evaluated by determination of nitric oxide production and 3-(4,5-dimethylthiazol-2-yl)-2,5-diphenyl tetrazolium bromide (MTT) test. The alveolar macrophages culture was tested in the presence of the κ -carrageenan/quercetin-Np multilayer coating and showed a cell viability of $91.3 \pm 9.6\%$. These results suggest that this multilayered coating is adequate for surfaces modification in view of biomedical and food industry applications.

Keywords Biomaterial · Cytotoxicity · Multilayer · Polyelectrolyte · Surface modification

Introduction

Multilayers films/coatings obtained by layer-by-layer (LbL) technique are considered important systems on the development of thin films, edible coatings, biomaterials, delivery sys-

tems of bioactive compounds and in modification of different surfaces (Liu et al. 2005; Peng et al. 2016; Chen et al. 2017; Gand et al. 2014; Medeiros et al. 2014; Souza et al. 2015a). This can be attributed to the extraordinary versatility and flexibility afforded by LbL technique, which make possible the production of multifunctional materials using a wide range of molecules, which are utilized as construction blocks, which self-organize through different types of interactions (electrostatic, hydrogen bonds, acid-base or coordination interactions, or even covalent bonds), making possible to obtain materials with different shapes, size, and composition (Guzmán et al. 2017). Another characteristic particularly attractive in the coatings obtained by LbL technique is the possibility of incorporating bioactive molecules during the assembly process, in order to confer a specific bioactivity, which opens a way for the development of promising materials with applications in different research areas (Pauthe and Tassel 2014).

The oxidative degradation is a limitative key factor in the shelf life of many foods and consumer products as well as in nutritional supplements. Many packaged products undergo deterioration of quality during transport and storage due to

✉ Maria G. Carneiro-da-Cunha
mgcc@ufpe.br

¹ Biochemistry Department, Universidade Federal de Pernambuco-UFPE, Av. Prof. Moraes Rego s/n, CEP 50, Recife, Pernambuco 670-420, Brazil
² LIKA - Laboratório de Imunopatologia Keizo Asami, UFPE, Cidade Universitária, CEP 50, Recife, Pernambuco 670-901, Brazil
³ CEB – Centre of Biological Engineering, Universidade do Minho, Campus de Gualtar, 4710-057 Braga, Portugal
⁴ Unidade Acadêmica de Medicina Veterinária, Universidade Federal de Campina Grande, CEP 58, Patos, Pernambuco 7000-970, Brazil
⁵ Present address: International Iberian Nanotechnology Laboratory-INL, Av. Mestre José Veiga s/n, 4715-330 Braga, Portugal

oxidative reactions that cause loss of nutritional and organoleptic properties such as lipid rancidity, color loss, and degradation of vitamins (Bastarrachea et al. 2015; Busolo and Lagaron 2015; Carrizo et al. 2016). One strategy that can be used for the preservation of oxidation-sensitive products is the development of films or coatings with antioxidant properties (Bastarrachea et al. 2015; Limpisophon and Schleining 2017). In the biomedicine field, the oxidative stress (a biological condition in which imbalance occurs between the production and elimination of free radicals) plays an important role in the limited biological compatibility of many biomaterials due to inflammation as well as in several pathologies, including atherosclerosis (Barbosa et al. 2010; Lith et al. 2014). Consequently, biomaterials capable to fight against the oxidative stress effects and inhibiting the excessive generation of free radicals can be useful tools.

Polyphenolic compounds can directly scavenge reactive oxygen species (ROS) by donating one of their delocalized electrons or hydrogen atoms due to both their acidic nature and ability to transfer electrons while remaining relatively stable (Busolo and Lagaron 2015). Quercetin represents the most abundant dietary flavonoid found in a broad range of fruits, vegetables, and beverages, whose antioxidant and anti-inflammatory properties have been associated with the prevention and therapy of cardiovascular diseases and cancer (Russo et al. 2012). With the purpose to improve the bioactivity and the molecular stability of quercetin against possible adverse conditions during processing, distribution, storage, and consumption of food products, quercetin was encapsulated by our group as lecithin/chitosan nanoparticles using the self-assembly technique (Souza et al. 2014). Nanoparticles presented a spherical morphology with an average size of 168.58 ± 20.94 nm, ζ -potential of $+56.46 \pm 1.94$ mV and showed improved antioxidant properties in comparison with free-quercetin.

Carrageenan is a natural carbohydrate (polysaccharide) obtained from edible red seaweeds and is a sulfated polygalactan with 15 to 40% of ester-sulfate content and an average relative molecular mass above 100 kDa. Carrageenan is formed by alternate D-galactose and 3,6-anhydro-galactose (3,6-AG) joined by α -1,3 and β -1,4-glycosidic linkage and can be classified into several types (λ , κ , ι , ϵ , μ) containing about from 22 to 35% sulfate groups. The kappa-carrageenan type presents an ester sulfate content from 25 to 30% and a 3,6-AG content of about 28 to 35% (Necas and Bartosikova 2013). Due to its high hydrophilicity, mechanical strength, biocompatibility, biodegradability, and absence of toxicity, this polymer has been mostly used in the food industry as gelling, stabilizing, and thickener agent (Albuquerque et al. 2016).

The κ -carrageenan gelling capability is the result of a coil-helix transition and subsequent helical aggregation. The gelation process is sensitive to κ -carrageenan concentration, temperature, addition of sugars, salt, and polyols (Yang et al. 2018; Liu and Li 2016; Stenner et al. 2016). Recently, κ -

carrageenan has been explored as template for oleogel preparation; κ -carrageenan aerogels resulted to be highly porous and structurally stable materials with high mechanic strength and capacity to uptake large amounts of oil, thus making them suitable to be used in the food, pharmaceutical, or cosmetic industries for pioneering applications (Manzocco et al. 2017). Nanolayered coatings based on κ -carrageenan and chitosan obtained by layer-by-layer deposition technique exhibit good gas barrier properties and therefore offer great potential to be used to coat food systems (Pinheiro et al. 2012). A nanolayered coating of κ -carrageenan and lysozyme assembled on pears' surface had a significant positive effect on the quality of the fruits and therefore hold potential for their shelf life extension (Medeiros et al. 2012).

The present work comes in the sequence of our previous achievements, aiming at the construction and characterization of a multilayer coating based on κ -carrageenan and quercetin-loaded lecithin/chitosan, by the LbL technique, and the evaluation of its antioxidant capacity and potential cytotoxicity *in vitro*.

Material and Methods

Material

Kappa-carrageenan (MW = 3.8×10^5 Da, 76% purity, Genugel carrageenan type WR-78) was purchased from CPKelco (Denmark), soya lecithin (Lipoid S45) from Lipoid (Ludwigshafen, Germany), chitosan (90% deacetylation, MW = 3.4×10^5 Da) from Aqua Premier Co. Ltd. (Thailand), and polyethylene terephthalate (PET) sheets from Canson (Annonay Cedex, France). Solvents used were of analytical grade and obtained from Merck (Darmstadt, Germany). All other reagents were purchased from Aldrich (Steinheim, Germany). The water was purified through a Millipore Q purification system (Millipore Corp., Bedford, MA).

Preparation of Polyelectrolyte Solutions

The κ -carrageenan 0.4% (w/v) solution was prepared under magnetic stirring at approximately 200 rpm for 4 h at room temperature (25 °C). The pH of solution was adjusted to 7.0 with 1 M sodium hydroxide.

Quercetin-loaded lecithin/chitosan nanoparticles were prepared according to Souza et al. (2014). Briefly, the nanoparticle suspension was obtained by dropwise injection (syringe with 0.38 mm internal diameter, 1 mL min⁻¹ injection rate) of 2 mL of ethanolic solution of Lipoid S45 (25 mg/mL) with quercetin (70 μ g/mL) in 23 mL aqueous solution of chitosan (0.11 mg/mL) under mechanical stirring (24,000 rpm, TP 18/10-10 N Ultraturrax, IKA Werke, Staufen, Germany). Chitosan aqueous solution was prepared diluting a standard solution of 0.2% (w/v) chitosan in 1.0% (v/v) lactic acid. The

nanoparticle suspension was termed quercetin-Np, and its final pH was adjusted to 3.3.

Quercetin-Np Size

The hydrodynamic diameter (size-average) and polydispersity index (PDI) of quercetin-Np were determined by dynamic light scattering (DLS) (Zetasizer Nano ZS, Malvern Instruments, UK). The samples were diluted (1:3 v/v) with Milli-Q water (Milli-Q synthesis, 18.2 MΩ cm) and analyzed in a folded capillary cell. Scattered light detection was carried out at 173° (NIBS=non-invasive backscatter detection) to reduce the path length of the scattered light from the samples and to minimize the risk of multi-scattering at 25 °C. All measurements were carried out in triplicate with three readings for each of them. The results were expressed as average ± standard deviation of nine values obtained.

Zeta Potential

ζ-potential of κ-carrageenan solution and quercetin-Np were measured at room temperature (25 °C) in a folded capillary cell by laser doppler micro-electrophoresis using a Zetasizer ZS Nano (Zetasizer Nano ZS, Malvern Instruments, UK) (Pinheiro et al. 2012 and Souza et al. 2014). All measurements were carried out in triplicate with three readings for each of them. The results were expressed as average ± standard deviation of nine values obtained.

Multilayer Coating Preparation

Polyethylene terephthalate (PET) sheets, used as support, were cut into rectangular pieces of 0.8 cm × 5.0 cm for UV-Vis, contact angle, scanning electron microscopy (SEM), atomic force microscopy (AFM), and antioxidant activity analyses and into circular pieces of a 35-mm diameter for cytotoxicity activity evaluation, and aminolyzed according to Fu et al. (2005) and Carneiro-da-Cunha et al. (2010). The PET sheet surface was treated by chemical aminolysis method using 1,6-hexanediamine to insert amino groups, through a nucleophilic attack of nitrogen to carbonium center of the carbonyl ester. These random attacks on the carbonyl groups of the polymer molecule present on the sheet surface generate and remove short chains. The aminolyzed PET was subsequently treated with HCl (0.1M) to charge positively the PET surface and termed as aminolyzed/charged PET (A/C PET). This procedure was necessary to charge positively the otherwise neutral PET surface to assure a stronger interaction with the negatively charged κ-carrageenan.

A/C PET pieces were immersed into κ-carrageenan solution (pH 7.0) for 15 min and subsequently rinsed with distilled water with pH 7.0 and dried with a nitrogen flow. Afterwards, the A/C PET pieces with the first layer adsorbed were immersed into the quercetin-Np suspension (pH 3.3) for 15 min and subsequently rinsed with distilled water with pH 3.3 and dried again with a

nitrogen flow. This process was repeated until the alternate deposition of a total of five layers (three κ-carrageenan and two quercetin-Np layers) was achieved.

Multilayer Coating Characterization

UV-Vis Spectroscopy

To follow the multilayer coating assembly was used a UV-Vis spectrophotometer (Jasco 560, Germany) to measure the absorbance of successive layers at a wavelength of 260 nm for κ-carrageenan layers according to Pinheiro et al. (2012) and at 373 nm for quercetin-Np layers according to Souza et al. (2014). Three replicates of each measurement were obtained.

Contact Angle

Contact angles (θ) of original PET, A/C PET, and of the subsequent five layers' surface were measured in a contact angle meter (OCA 20, Dataphysics, Germany) using the sessile drop method (Newman and Kwok 1999). A 2-μL droplet of ultrapure water was placed on the horizontal surface with a 500 μL syringe (Hamilton, Switzerland) with a needle of a 0.75-mm diameter. Measurements were made at 15 s, and for each type of surface, three samples were used. For each sample, ten contact angle measurements were carried out at 18 ± 0.3 °C.

Surface Analysis

The surface morphology of the multilayers was observed and analyzed by scanning electron microscopy (SEM, Nova 130 NanoSEM 200, The Netherlands) and by atomic force microscopy (AFM, Witec alpha300, Germany).

SEM was carried out with an accelerating voltage from 10 to 15 kV. Before being analyzed, all samples were mounted on aluminum stubs using carbon adhesive tape and sputter-coated with gold (thickness of about 10 nm).

The AFM was equipped with nitride AFM CLA-10 probe type PNP-DB, with a resonance frequency of 17–67 kHz and force constant of 0.06–0.48 N/m. AFM images were analyzed using WITec Project and Gwyddion software. The roughness average (Ra) and roughness root mean square (RMS) values were calculated across 5 μm × 5 μm areas (Kononova et al. 2018; Fu et al. 2005; Liu et al. 2017). The mathematical definition and the digital implementation of these parameters were carried out as follows (Gadelmawla et al. 2002):

$$Ra = \frac{1}{n} \sum_{i=1}^n |Y_i| \quad (1)$$

$$RMS = \sqrt{\frac{1}{n} \sum_{i=1}^n Y_i^2} \quad (2)$$

where n in the equation corresponds to the number of intersections of the profile at the mean line and y represents height variations.

Antioxidant Activity

For antioxidant activity evaluation of the multilayer coating, two techniques were used—2,2-diphenyl-1-picrylhydrazyl (DPPH) and Ferric Reducing Antioxidant Power (FRAP) according to Souza et al. (2014), with small adjustments and adapted for solid samples. Briefly, rectangular samples of A/C PET (control) and coated A/C PET (sample), 0.8 cm × 5.0 cm in size, were pre-cut transversely in the middle and the two pieces obtained were placed into a 35-mm diameter well of 6-well dishes, containing related reagent solutions.

For DPPH, samples were immersed into wells with 2 mL of ethanolic solution of DPPH (200 μM) and the mixture was gently shaken for 30 min at room temperature (25 °C) in the dark. Subsequently, the reaction solution was transferred to 96-well dishes and the absorbance measured at 515 nm (ELISA reader; Bio-Rad). In DPPH radical form, this molecule has an absorbance peak at 515 nm that disappears with the acceptance of an electron from an antioxidant compound to become a stable diamagnetic molecule. The scavenging percentage of free radicals by the sample was calculated according to the following equation: Scavenging capacity (%) = $[(1 - \text{Abs}_{515\text{sample}}) / \text{Abs}_{515\text{control}}] \times 100$, where $\text{Abs}_{515\text{sample}}$ is the absorbance of the coated A/C PET and $\text{Abs}_{515\text{control}}$ is the absorbance of A/C PET. All determinations were carried out in triplicate and results expressed as average ± standard deviation.

For the FRAP assay, the samples were immersed into wells with 2 mL of FRAP reagent and the mixture was subsequently incubated at 37 °C for 15 min and, after that, transferred to 96-well dishes and the absorbance determined at 593 nm (ELISA reader; Bio-Rad). A calibration curve was prepared with $\text{FeSO}_4 \cdot 7\text{H}_2\text{O}$ (50–1500 μM) as standard. FRAP reagent was freshly prepared mixing 10 mM 2,4,6-tris(1-pyridyl)-5-triazine (TPTZ) in 40 mM HCl with a 20 mM FeCl_3 solution and 0.3M acetate buffer (pH 3.6) in the proportion 1:1:10 (v/v/v). The results expressed as micrometer of ferrous equivalent Fe^{2+} from the average of three replicates ± standard deviation.

In Vitro Cytotoxicity

To evaluate the cytotoxicity of the multilayer coating, nitric oxide (NO) production, and cell viability by MTT (3-(4,5-dimethylthiazol-2-yl)-2,5-diphenyl tetrazolium bromide) tests in cultures of alveolar macrophages were used. The NO and MTT tests evaluate, respectively, the oxidative stress and the percentage of viable cells after contact with the material; therefore, they are tests that produce complementary responses.

Animals

Alveolar macrophages were obtained from male Wistar rats (90 days old, weighting 250–300 g). The animals were kept under controlled condition ad libitum access to water and food, 12-h light–dark cycle and at 20 °C room temperature during at least 1 week before any experimental manipulation. All experiments with rats were approved by Comitê de Ética em Experimentação Animal do Centro de Biociências of the Universidade Federal de Pernambuco (process no. 23076.018849/2012-01) and follow the Norms of Colégio Brasileiro de Experimentação com Animais (COBEA).

Bronchoalveolar Lavage Fluid

The methodology used to obtain the bronchoalveolar lavage (BAL) fluid was carried out according to De Castro et al. (1995). The animals were intraperitoneally anesthetized with 0.5% (w/v) chloralose and 12.5% (w/v) urethane in the proportion of 8 mL/kg. Alveolar macrophages were recovered with the aid of a plastic cannula previously inserted into rats' trachea. BALs were carried out using 0.9% (w/v) NaCl injected into the cannula using a syringe, at room temperature. In this way, several aliquots of 5 mL were injected, followed by recovery, and placed in a 15 mL conical polypropylene tube (Falcon, Sigma). The BAL fluid recovery was of approximately 30 mL for each animal; the content was then centrifuged (10 min, 470 × g) and the cells from the pellets were finally pooled.

Culture of Alveolar Macrophages

The cell' pellets obtained from centrifuged BAL fluid were resuspended in a culture medium (Roswell Park Memorial Institute-RPMI 1640, Gibco) supplemented with heat-inactivated fetal calf serum (3%, Gibco), penicillin (100 U/mL), streptomycin (100 mg/mL), and amphotericin B (0.25 mg/mL), all from Sigma (USA). One milliliter of the suspension (10^6 cells/mL) was transferred into each of the 35-mm diameter wells of a 6-well dish, where no samples (i.e., without A/C PET) and samples of A/C PET and of coated A/C PET were previously placed. They were allowed to adhere for 1 h at 37 °C in a humidified atmosphere containing 5% CO_2 . Non-adherent macrophage cells were discarded and the remaining monolayers (>95% adherent macrophage) were used in the subsequent tests.

Nitric Oxide

Nitric oxide is a regulatory molecule that can be produced by macrophages after stimulation and presents great importance in processes of the immune response, inflammation, and apoptosis. For this reason, a clear understanding of the complex

interaction between macrophages and biomaterials is important for the improvement of materials employed in the construction of biomedical devices (Kao 1999).

The nitric oxide (NO) production was determined indirectly by nitrite and nitrate quantification in macrophage culture supernatant (liquid phase) collected of the 6-well dishes, according to the method described by Feder and Laskin (1994). One milliliter of the culture medium (RPMI) was added to the adhered macrophage cultures obtained as mentioned in subsection 2.8.3., and 10 μL of NaCl 0.9% (w/v) or 10 μL of *Escherichia coli* lipopolysaccharide-LPS (1 mg/mL) was added in the wells where no samples were previously placed (i.e., without A/C PET and coated A/C PET). In this way, the test was carried out with four different groups: A/C PET, coated A/C PET, negative control (NaCl), and positive control (*Escherichia coli* lipopolysaccharide-LPS). After 24 h of incubation in contact with the samples, 500 μL of the supernatant of the macrophage culture was removed from a test tube and was added with 500 μL of the Griess reagent (solution 1:1 of 1.0% (w/v) sulfanilamide in 5.0% (w/v) H_3PO_4 and 0.1% (w/v) Naphthylethylene diamine dihydrochloride). Then, the mixture was incubated at 37 °C for 10 min and the absorbance was measured in an ELISA reader (Bio-Rad, model 550) at 540 nm. The nitrite concentration was calculated with the aid of a NaNO_2 standard curve (12.5 μM –10.0 mM) and the data expressed in mMol of nitrite. The average value of five samples \pm standard deviation was used as final result.

Cell Viability

Cell activity was determined by MTT (3-(4,5-dimethylthiazol-2-yl)-2,5-diphenyl tetrazolium bromide) test (Mosmann 1983), aiming and evaluating the cellular viability of the macrophages in the presence of this new material. After supernatant removal from the four groups of macrophage cultures used in the NO test (A/C PET, coated A/C PET, negative control (10 μL NaCl 0.9% w/v), and positive control (10 μL of *Escherichia coli* lipopolysaccharide-LPS at 1 mg/mL)), cells were washed with PBS (0.01 M, pH 7.0) and, afterwards, added 500 μL of the MTT (1 mg/mL culture medium RPMI) solution with subsequent incubation at 37 °C for 3 h. The supernatant was removed again and 500 μL of dimethyl sulfoxide (DMSO) were added to the cells in order to solubilize the formazan crystals with the aid of a scraper. Absorbance values were measured by a microplate reader (Bio-Rad, model 550) at a wavelength of 570 nm, using DMSO as blank. Five replicates were carried out for each sample and the average value \pm standard deviation were used as final result.

The results were expressed in percentage of cell viability according to the following equation: Cell viability (%) = $(\text{Abs}_{570\text{s}}/\text{Abs}_{570\text{b}}) \times 100$, where $\text{Abs}_{570\text{s}}$ is the

sample absorbance and $\text{Abs}_{570\text{b}}$ the blank absorbance (wells containing only cells).

Statistical Analyses

Where appropriate, data are presented as average with standard deviations (SD) as error bars, calculated over three or more data points. Significant differences between two groups were evaluated by Student's *t* test and between more than two groups by one-way analysis of variance (ANOVA), followed by Tukey's test in GraphPrism® (GraphPad Software Inc., San Diego, CA). The level of significance was set at $p < 0.05$.

Results and Discussion

Polyelectrolyte Characterization

The quercetin-Np showed a size of 160.3 ± 1.94 nm with low polydispersity index ($\text{PDI} = 0.25 \pm 0.01$), which features a reasonably homogeneous suspension. This result is in agreement with that reported by Souza et al. (2014) (168.58 ± 20.94) for the same type of nanoparticle containing 70 μg of quercetin/mL suspension.

The electrostatic properties of κ -carrageenan solution and of quercetin-Np suspension were confirmed by determination of their ζ -potential, in order to ensure the possibility of establishing interaction between the support surface (A/C PET) and the first κ -carrageenan layer, and subsequently between successive layers during the multilayer coating self-assembly.

The ζ -potential value obtained for κ -carrageenan solution was found to be -53.33 ± 3.23 mV at pH 7.0 and for quercetin-Np suspension $+59.66 \pm 0.73$ mV at pH 3.3, confirming the opposite charges of these two polyelectrolytes. These values mean that these polyelectrolytes can interact by electrostatic forces. The κ -carrageenan value was similar to those found by Pinheiro et al. (2012) (-56.90 ± 5.11 mV at pH 7.0) and Medeiros et al. (2012) (-60.53 ± 0.15 mV at pH 7.0). The value of pH chosen here (pH = 7.0) was chosen based on κ -carrageenan's dissociation constant ($\text{p}K_{\text{a}} = 2.0$) (Jones et al. 2010) to ensure a negative ζ -potential value and its stronger interaction with the A/C PET surface, charged positively.

The positive ζ -potential value of quercetin-Np is in agreement with the value reported by Souza et al. (2014) ($+56.46 \pm 1.94$ mV) and can be justified by the presence of positively charged amino groups of chitosan present on the surface of quercetin-Np at pH 3.3. Thus, the amino groups of chitosan layer, protonated at pH 3.3, are responsible for the high positive ζ -potential of quercetin-Np since the phosphate groups (PO_3^-) of lecithin ($\text{p}K_{\text{a}} \sim 1.5$) and the amino groups (NH_3^+) of chitosan ($\text{p}K_{\text{a}} \sim 6.2$ –7.0) have opposite charges. This suggests

that a protective chitosan layer around the quercetin-Np particles is formed through electrostatic interactions.

UV-Vis Spectroscopy

Figure 1 shows the absorbance evolution with each successive layer deposition, suggesting that similar amounts of polyelectrolytes were adsorbed and confirming the assembly success. The multilayer coating spectra exhibited a maximum absorbance at 260 nm for the κ -carrageenan layers and at 373 nm for the quercetin-Np layers. The κ -carrageenan deposition at 260 nm in the κ -carrageenan/chitosan layered coating was also observed by Pinheiro et al. (2012). The absorption band at 373 nm for quercetin-Np is arising from the conjugations in the A-ring of the quercetin molecule such as described by Souza et al. (2014). The increase in the absorbance due to the layers' deposition have been also described by other authors that used layer-by-layer deposition technique characterized by UV-Vis spectroscopy (Peng et al. 2016; Medeiros et al. 2014; Pinheiro et al. 2012; Carneiro-da-Cunha et al. 2010; Fu et al. 2005).

Contact Angle

Figure 2 displays the contact angle values found on PET, A/C PET and on successive adsorbed layers, disclosing the well-succeeded assembled coating, with same oscillation behaviors also found by other authors (Fabra et al. 2016; Medeiros et al. 2014; Pinheiro et al. 2012; Medeiros et al. 2012; Carneiro-da-Cunha et al. 2010). Due to aminolysis, the A/C PET contact angle value ($\theta \sim 65^\circ$) is slightly lower than that of the original PET ($\theta \sim 73^\circ$). The quercetin-Np layer exhibited a contact angle ($\sim 50^\circ$) which is approaching the values of surfaces with hydrophobic nature ($\theta > 70^\circ$); in contrast, the contact angle value found for the

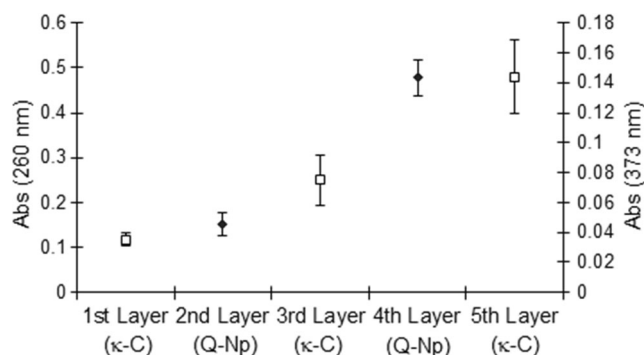


Fig. 1 UV-Vis spectroscopy analysis of five successive layers. Square represents the wavelength of 260 nm for κ -carrageenan (κ -C) and diamond at 373 nm for quercetin-Np (Q-Np). Each data point is an average of three determinations, and the error bars show the standard deviation

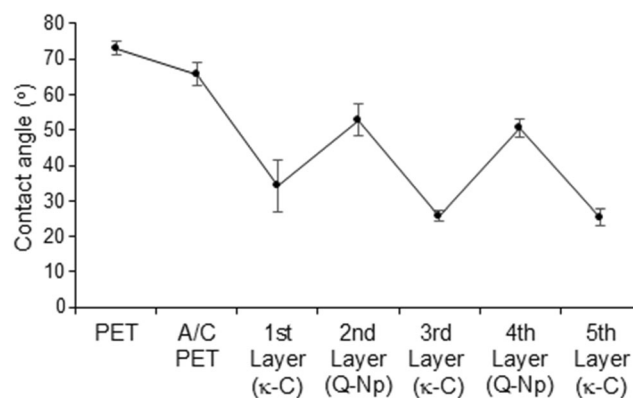


Fig. 2 Contact angle measurement on original PET, A/C PET, and on five successive layers (κ -carrageenan (κ -C) and quercetin-Np (Q-Np)). Each data point is an average of ten measurements, and the error bars show the standard deviation

outermost κ -carrageenan layer ($\theta \sim 25^\circ$) is quite close to that of hydrophilic (wetable) surfaces ($\theta < 20^\circ$). Being the last (5th) layer a κ -carrageenan one, the whole multilayer system exhibited a relatively hydrophilic characteristic. This means that it is possible to tailor the hydrophobicity/hydrophilicity of a multilayer system as a function of the polyelectrolyte that is placed on the last layer.

Surface Analysis

The surface morphology of A/C PET, examined by SEM (Fig. 3a), showed changes after the addition of different layers by layer-by-layer assembly (Fig. 3b–i). These results, also confirmed by UV-Vis and contact angle, suggest the successful assembly of the coating. All κ -carrageenan layers (Fig. 3b, d, and f) show a more flat and homogeneous morphology than quercetin-Np layers. The κ -carrageenan surface morphology is similar to that observed by Pinheiro et al. (2012) on κ -carrageenan/chitosan nanocoatings. Figure 3c, e, corresponding to quercetin-Np layers, shows the presence of dense structures and wells unevenly distributed on the surface. It is also possible to observe a marked roughness of the 4th layer (Fig. 3e), probably due to the presence of spherical structures, similar to quercetin-Np (Fig. 3h), also observed by Souza et al. (2014). Figure 3g–i shows the SEM cross-sectional images of the multilayer structure (Fig. 3g, h, and i correspond to the 1st, 3rd, and 5th layers, respectively). Figure 3i allowed to roughly estimate the coating thickness to be of around 182.5 nm, a similar dimension (198.2 nm) to the one found by Medeiros et al. (2014).

AFM analysis was carried out in order to obtain further information about surface roughness on A/C PET with the polyelectrolyte deposition; Fig. 4 shows the corresponding 3D topographical images. A surface morphology change was observed when the layers were deposited on the A/C PET support. The roughness average (Ra) and roughness root

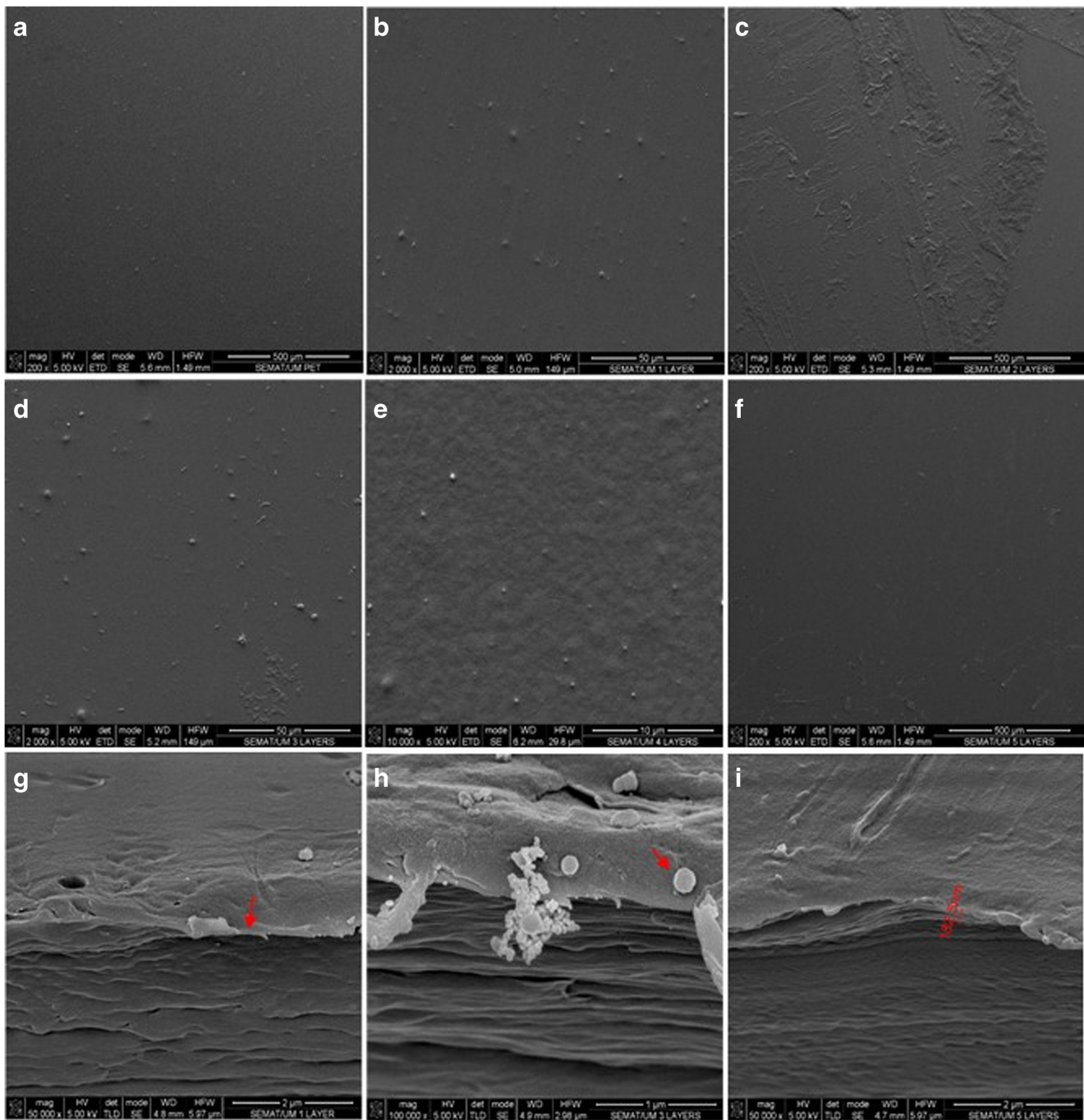


Fig. 3 SEM surface morphology images. **a** A/C PET, **b** first layer of κ -carrageenan, **c** coating with two layers (κ -carrageenan and quercetin-Np), **d** coating with three layers (κ -carrageenan, quercetin nanoparticles, and

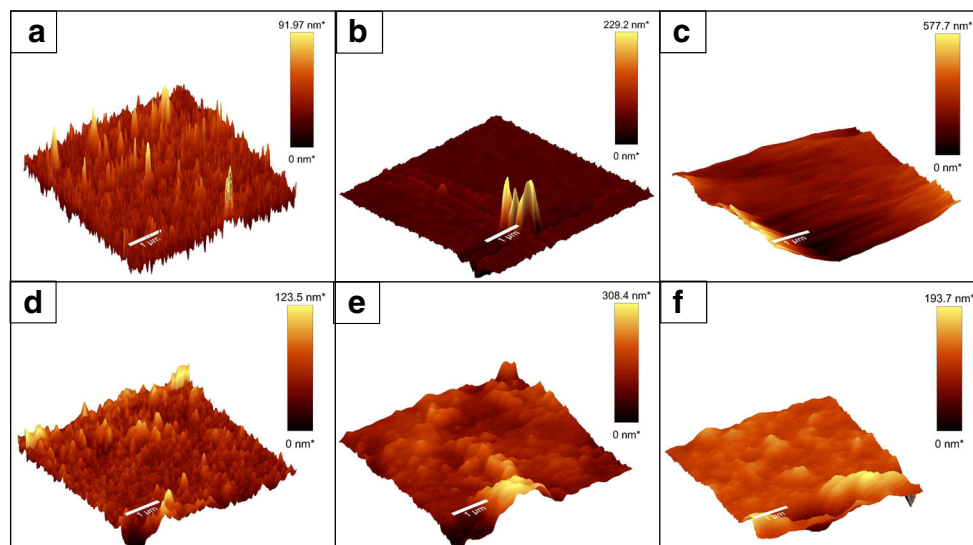
κ -carrageenan), **e** coating with four layers, **f** coating with five layers, **g** cross-sectional SEM image of the 1st layer, **h** cross-sectional SEM image of the three layer, and **i** cross-sectional SEM image of the five layers

mean square (RMS) values for A/C PET and five layers were calculated across $5 \mu\text{m} \times 5 \mu\text{m}$ areas (Table 1). As expected from the direct observation of the images, the layers formed by quercetin-Np (layers 2nd and 4th) presented higher roughness values than the layers formed by κ -carrageenan (layers 1st, 3rd, and 5th), reflecting a lower homogeneity in the deposition of quercetin-Np on the surface, possibly due to its lower hydrophilicity.

Antioxidant Activity

The DPPH results showed that κ -carrageenan/quercetin-Np multilayer coating can scavenge free radicals by reduction of the DPPH• radicals with a scavenging activity of $31.32 \pm 3.13\%$. Souza et al. (2015b) reported a DPPH scavenging capacity of quercetin-chitosan films of approximately 64%, which was higher than that obtained in this work. However,

Fig. 4 AFM surface morphology images: **a** A/C PET, **b** coating with first layer of κ -carrageenan, **c** coating with 2nd layer, **d** coating with 3rd layer, **e** coating with 4th layer, and **f** coating with 5th layer



it is important to highlight the different quercetin concentrations of each work: the nanoparticles produced in this work contained only $70 \mu\text{g mL}^{-1}$, whereas in the quercetin-chitosan films, it was $200 \mu\text{g mL}^{-1}$. The obtained FRAP results were $799.41 \pm 95.39 \mu\text{M}$ of ferrous equivalent Fe^{2+} , demonstrating that the multilayer coating also played a role as an electron-donating antioxidant in the change of the ferric complex (Fe^{3+} -tripirydyltriazine) by a ferrous complex (Fe^{2+} -tripirydyltriazine). Souza et al. (2014) showed that the antioxidant capacity of quercetin was increased after the encapsulation in lecithin/chitosan nanoparticles (quercetin-Np) and improved its dissolution properties. In our work, it is possible to observe that, even after the immobilization of quercetin-Np in a multilayer coating, this antioxidant effect was preserved. This behavior shows that the antioxidant performance of the multilayer coating is based on the capacity of quercetin's phenolic group (contained in nanoparticles) to donate hydrogen as free radical scavenger since the A/C PET support and κ -carrageenan are not able to donate active hydrogen atoms or transfer electrons to reduce DPPH or Fe^{3+} . Consequently, the chemical structure of the layers used was an important factor

to obtain antioxidant activity in multilayer coating (Ebrahimi et al. 2015). Vera et al. (2016) incorporated selenium nanoparticles (SeNPs) in a multilayer food packaging material based in a plastic structure of PET-Adhesive-low-density polyethylene, obtaining a new antioxidant material. The antioxidant capacity was based on the action of SeNPs as free radicals' scavengers.

In Vitro Cytotoxicity

Nitric Oxide (NO)

One of the main parameters for the evaluation of biological response and of damages or cell death potential is the cytotoxicity tests, which are the first trial tests used for almost all the materials (Toledo et al. 2012). Macrophages are cells that upon contact with an aggressive agent, act by releasing cytokines and pro-inflammatory mediators that initiate and amplify the inflammatory process. These cells are part of the immune system and are closely related to immune responses, inflammation, and foreign body, such as physical, chemical, or bacterial aggressor stimulus (Xia and Triffitt 2006).

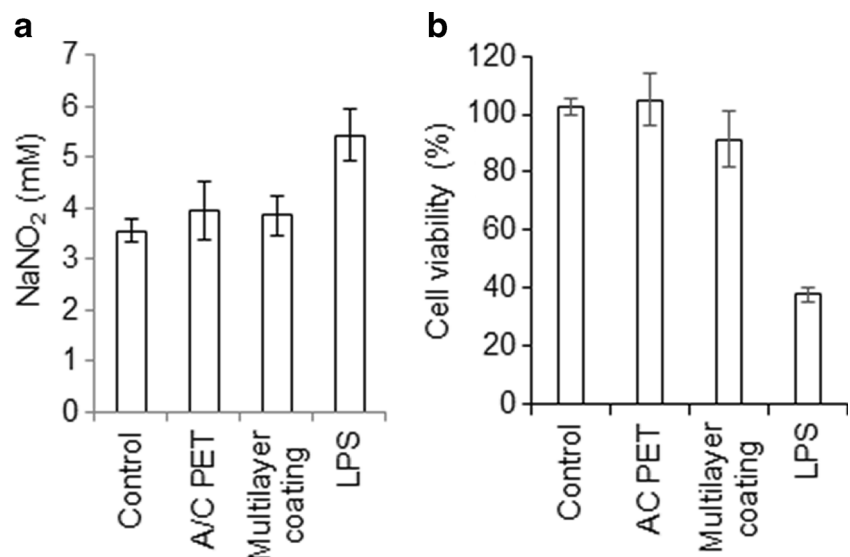
Figure 5a shows the results of the production of nitric oxide by macrophages exposed to A/C PET and multilayer coating, together with the negative ($\text{NaCl } 0.9\% \text{ w/v}$) and positive controls (*E. coli* LPS). The systems stimulated by A/C PET and multilayer coating produced similar concentrations of nitric oxide which were compatible with that presented by the negative control ($p < 0.05$), which contained only macrophages in culture, and quite different from that produced by the positive control, due to macrophage activation by LPS. These results showed that these materials did not cause damage to cells, demonstrating to be not toxic, as proved by the similarity of the initial viability of the macrophages used in the control culture.

Table 1 Roughness of A/C PET and polyelectrolytes layers

Surface	Ra (nm)	RMS (nm)
A/C PET	101.5	147.1
1st layer (κ -Carrageenan)	75.0	158.2
2nd layer (Quercetin-Np)	138.4	187.6
3rd layer (κ -Carrageenan)	111.6	156.4
4th layer (Quercetin-Np)	126.4	166.4
5th layer (κ -Carrageenan)	65.1	109.6

Ra roughness average, RMS roughness root mean square

Fig. 5 In vitro cytotoxicity of A/C PET and multilayer coating: **a** Nitric oxide production and **b** cell viability by MTT test



Cell Viability

In order to verify the cell viability of macrophage cultures exposed to κ -carrageenan/querctin-Np multilayer coating, the MTT reduction test was used because it is a simple and extremely useful in vitro method to evaluate the biocompatibility of new materials. The results showed values of cell viability of $104.8 \pm 8.8\%$ and $91.3 \pm 9.6\%$, respectively, for A/C PET and κ -carrageenan/querctin-Np multilayer coating, which were not significantly different ($p < 0.05$) from the negative control ($102.5 \pm 2.8\%$) after 24 h of culture (Fig. 5b). These results demonstrate that the coating does not interfere with the cellular metabolism, being thus in agreement with those obtained with the NO test. However, as expected, the LPS (positive control) showed a significantly lower cell viability ($38.0 \pm 2.4\%$), being considered cytotoxic according to ISO 10993-5 2009, which considers a potentially cytotoxic product when it reduces cell viability at rates lower than 70%. In this way, we can conclude that κ -carrageenan/querctin-Np multilayer coating and A/C PET have the ability to support the viability and proliferation of macrophages, both exhibiting comparable biocompatibility.

Conclusions

The present work allows concluding that a multilayer coating containing κ -carrageenan and querctin-Np was successfully built by the layer-by-layer technique, which is easy to scale-up aiming at future industrial applications. Here, we show that the developed system may be adapted for application to a large variety of surface types. The new multilayer coating had good antioxidant activity, did not present cytotoxicity, and could thus be considered as potentially biocompatible. In this way, this technology can be a viable tool for the

biomedical and food industries, with the potential to provide biocompatibility to different surfaces, as well as to be used in the development of active packaging materials, e.g., with the objective of prolonging the shelf life of food products.

Acknowledgements This work was supported by the Portuguese Foundation for Science and Technology (FCT) under the scope of the strategic funding of UID/BIO/04469/2013 unit, and COMPETE 2020 (POCI-01-0145-FEDER-006684) and BioTecNorte operation (NORTE-01-0145-FEDER-000004) funded by the European Regional Development Fund under the scope of Norte2020 - Programa Operacional Regional do Norte. The authors would also like to thank the Brazilian Government for support given by the Conselho Nacional de Desenvolvimento Científico e Tecnológico (CNPq). Carneiro-da-Cunha, M.G. expresses her gratitude to the CNPq for research grant.

References

- Albuquerque, P. B. S., Coelho, L. C. B. B., Teixeira, J. A., & Carneiro-da-Cunha, M. G. (2016). Approaches in biotechnological applications of natural polymers. *AIMS Molecular Science*, 3(3), 386–425. <https://doi.org/10.3934/molsci.2016.3.386>.
- Barbosa, K. B. F., Costa, N. M. B., Alfenas, R. C. G., De Paula, S. O., Minim, V. P. R., & Bressan, J. (2010). Oxidative stress: concept, implications and modulating factors. *Brazilian Journal of Nutrition*, 23(4), 629–643.
- Bastarrachea, L. J., Wong, D. E., Roman, M. J., Lin, Z., & Goddard, J. M. (2015). Active packaging coatings. *Coatings*, 5, 771–791.
- Busolo, M. A., & Lagaron, J. M. (2015). Antioxidant polyethylene films based on a resveratrol containing clay of interest in food packaging applications. *Food Packaging and Shelf Life*, 6, 30–41. <https://doi.org/10.1016/j.fpsl.2015.08.004>.
- Carneiro-da-Cunha, M. G., Cerqueira, M. A., Souza, B. W. S., Carvalho, S., Quintas, M. A. C., Teixeira, J. A., et al. (2010). Physical and thermal properties of a chitosan/alginate nanolayered PET film. *Carbohydrate Polymers*, 82(1), 153–159. <https://doi.org/10.1016/j.carbpol.2010.04.043>.
- Carrizo, D., Taborda, G., Nerín, C., & Bosetti, O. (2016). Extension of shelf life of two fatty foods using a new antioxidante multilayer packaging containing green tea extract. *Innovative Food Science*

- and Emerging Technologies, 33, 534–541. <https://doi.org/10.1016/j.ifset.2015.10.018>.
- Chen, W., Shen, X., Hu, H., Xu, K., Ran, Q., Yu, Y., et al. (2017). Surface functionalization of titanium implants with chitosan-catechol conjugate for suppression of ROS-induced cells damage and improvement of osteogenesis. *Biomaterials*, 114, 82–96. <https://doi.org/10.1016/j.biomaterials.2016.10.055>.
- De Castro, C. M. M. B., Nahori, M. A., Dumarey, C. H., Vargaftig, B. B., & Bachelet, M. (1995). Fenspiride: an anti-inflammatory drug with potential benefits in the treatment of endotoxemia. *European Journal of Pharmacology*, 294(2-3), 669–676. [https://doi.org/10.1016/0014-2999\(95\)00608-7](https://doi.org/10.1016/0014-2999(95)00608-7).
- Ebrahimiasl, S., Zakaria, A., Kassim, A., & Basri, S. N. (2015). Novel conductive polypyrrole/zinc oxide/chitosan bionanocomposite: synthesis, characterization, antioxidant, and antibacterial activities. *International Journal of Nanomedicine*, 10, 217–227. <https://doi.org/10.2147/IJN.S69740>.
- Fabra, M. J., Flores-López, M. L., Cerqueira, M. A., Rodriguez, D. J., Lagaron, J. M., & Vicente, A. A. (2016). Layer-by-layer technique to developing functional nanolaminate films with antifungal activity. *Food and Bioprocess Technology*, 9(3), 471–480. <https://doi.org/10.1007/s11947-015-1646-1>.
- Feder, L. S., & Laskin, D. L. (1994). Regulation of hepatic endothelial cell and macrophage proliferation and nitric oxide production by GM-CSF, M-CSF, and IL-13 following acute endotoxemia. *Journal of Leukocyte Biology*, 55(4), 507–513. <https://doi.org/10.1002/jlb.55.4.507>.
- Fu, J., Ji, J., Yuan, W., & Shen, J. (2005). Construction of anti-adhesive and antibacterial multilayer films via layer-by-layer assembly of heparin and chitosan. *Biomaterials*, 26(33), 6684–6692. <https://doi.org/10.1016/j.biomaterials.2005.04.034>.
- Gadelmawla, E. S., Koura, M. M., Maksoud, T. M. A., Elewa, I. M., & Soliman, H. H. (2002). Roughness parameters. *Journal of Materials Processing Technology*, 123(1), 133–145. [https://doi.org/10.1016/S0924-0136\(02\)00060-2](https://doi.org/10.1016/S0924-0136(02)00060-2).
- Gand, A., Hindí, M., Chacon, D., Tassel, P. R. V., & Pauthe, E. (2014). Nanotemplated polyelectrolyte films as porous biomolecular delivery systems. *Biomater*, 4(1), e28823. <https://doi.org/10.4161/biom.28823>.
- Guzmán, E., Mateos-Maroto, A., Ruano, M., Ortega, F., & Rubio, R. G. (2017). Layer-by-layer polyelectrolyte assemblies for encapsulation and release of active compounds. *Advances in Colloid and Interface Science*, 249, 290–307. <https://doi.org/10.1016/j.cis.2017.04.009>.
- ISO 10993-5. (2009). *International standard for biological evaluation of medical devices—part 5: tests for in vitro cytotoxicity*.
- Jones, O., Decker, E. A., & McClements, D. J. (2010). Thermal analysis of β -lactoglobulin complexes with pectins or carrageenan for production of stable biopolymer particles. *Food Hydrocolloids*, 24(2-3), 239–248. <https://doi.org/10.1016/j.foodhyd.2009.10.001>.
- Kao, W. J. (1999). Evaluation of protein-modulated macrophage behavior on biomaterials: designing biomimetic materials for cellular engineering. *Biomaterials*, 20(23–24), 2213–2221. [https://doi.org/10.1016/S0142-9612\(99\)00152-0](https://doi.org/10.1016/S0142-9612(99)00152-0).
- Kononova, S. V., Volod'ko, A. V., Petrova, V. A., Kruchinina, E. V., Baklagina, Y. G., Chusovitin, E. A., & Skorik, Y. A. (2018). Pervaporation multilayer membranes based on a polyelectrolyte complex of λ -carrageenan and chitosan. *Carbohydrate Polymers*, 181, 86–92. <https://doi.org/10.1016/j.carbpol.2017.10.050>.
- Limpisophon, K., & Schleining, G. (2017). Use of gallic acid to enhance the antioxidant and mechanical properties of active fish gelatin film. *Journal of Food Science*, 82(1), 80–89. <https://doi.org/10.1111/1750-3841.13578>.
- Lith, R. V., Gregory, E. K., Yang, J., Kibbe, M. R., & Ameer, G. A. (2014). Engineering biodegradable polyester elastomers with antioxidant properties to attenuate oxidative stress in tissues. *Biomaterials*, 35(28), 8113–8122. <https://doi.org/10.1016/j.biomaterials.2014.06.004>.
- Liu, S., & Li, L. (2016). Thermoreversible gelation and scaling behavior of Ca^{2+} -induced κ -carrageenan hydrogels. *Food Hydrocolloids*, 61, 793–800. <https://doi.org/10.1016/j.foodhyd.2016.07.003>.
- Liu, Y., He, T., & Gao, C. (2005). Surface modification of poly(ethylene terephthalate) via hydrolysis and layer-by-layer assembly of chitosan and chondroitin sulfate to construct a cyto-compatible layer for human endothelial cells. *Colloids and Surfaces B: Biointerfaces*, 46(2), 117–126. <https://doi.org/10.1016/j.colsurfb.2005.09.005>.
- Liu, Q., Wu, J., Lim, Z. Y., Aggarwal, A., Yang, H., & Wang, S. (2017). Evaluation of the metabolic response of Escherichia coli to electrolysed water by ^1H NMR spectroscopy. *LWT - Food Science and Technology*, 79, 428–436. <https://doi.org/10.1016/j.lwt.2017.01.066>.
- Manzocco, L., Valoppi, F., Calligaris, S., Andreatta, F., Spilimbergo, S., & Nicoli, M. C. (2017). Exploitation of κ -carrageenan aerogels as template for edible oleogel preparation. *Food Hydrocolloids*, 71, 68–75. <https://doi.org/10.1016/j.foodhyd.2017.04.021>.
- Medeiros, B. G. S., Pinheiro, A. C., Teixeira, J. A., Vicente, A. A., & Carneiro-da-Cunha, M. G. (2012). Polysaccharide/protein nanomultilayer coatings: construction, characterization and evaluation of their effect on 'Rocha' pear (*Pyrus communis* L.) shelf-life. *Food and Bioprocess Technology*, 5(6), 2435–2445. <https://doi.org/10.1007/s11947-010-0508-0>.
- Medeiros, B. G. S., Souza, M. P., Pinheiro, A. C., Bourbon, A. I., Cerqueira, M. A., Vicente, A. A., & Carneiro-da-Cunha, M. G. (2014). Physical characterisation of an alginate/lysozyme nanolaminate coating and its evaluation on 'Coalho' cheese shelf life. *Food and Bioprocess Technology*, 7(4), 1088–1098. <https://doi.org/10.1007/s11947-013-1097-5>.
- Mosmann, T. (1983). Rapid colorimetric assay for cellular growth and survival: application to proliferation and cytotoxicity assay. *Journal of Immunological Methods*, 65(1-2), 55–63. [https://doi.org/10.1016/0022-1759\(83\)90303-4](https://doi.org/10.1016/0022-1759(83)90303-4).
- Necas, J., & Bartosikova, L. (2013). Carrageenan: a review. *Veterinárni Medicina*, 58(4), 187–205.
- Newman, A. W., & Kwok, D. Y. (1999). Contact angle measurement and contact angle interpretation. *Advances in Colloid and Interface Science*, 81(3), 167–249.
- Pauthe, E., & Tassel, P. R. V. (2014). Layer-by-layer films as biomaterials: bioactivity and mechanics. *Journal of Biomaterials Science*, 25(14-15), 1489–1501. <https://doi.org/10.1080/09205063.2014.921096>.
- Peng, L., Li, H., & Meng, Y. (2016). Layer-by-layer structured polysaccharides-based multilayers on cellulose acetate membrane: towards better hemocompatibility, antibacterial and antioxidant activities. *Applied Surface Science*, 401, 25–39.
- Pinheiro, A. C., Bourbon, A. I., Medeiros, B. G. S., Silva, L. H. M., Silva, M. C. H., Carneiro-da-Cunha, M. G., et al. (2012). Interactions between κ -carrageenan and chitosan in nanolayered coatings-structural and transport properties. *Carbohydrate Polymers*, 87(2), 1081–1090. <https://doi.org/10.1016/j.carbpol.2011.08.040>.
- Russo, M., Spagnuolo, C., Tedesco, I., Bilotto, S., & Russo, G. L. (2012). The flavonoid quercetin in disease prevention and therapy: facts and fancies. *Biochemical Pharmacology*, 83(1), 6–15. <https://doi.org/10.1016/j.bcp.2011.08.010>.
- Souza, M. P., Vaz, A. F. M., Correia, M. T. S., Cerqueira, M. A., Vicente, A. A., & Carneiro-da-Cunha, M. G. (2014). Quercetin-loaded lecithin/chitosan nanoparticles for functional food applications. *Food and Bioprocess Technology*, 7(4), 1149–1159. <https://doi.org/10.1007/s11947-013-1160-2>.
- Souza, M. P., Vaz, A. F. M., Cerqueira, M. A., Teixeira, J. A., Vicente, A. A., & Carneiro-da-Cunha, M. G. (2015a). Effect of an edible nanomultilayer coating by electrostatic self-assembly on the shelf life of fresh-cut mangoes. *Food and Bioprocess Technology*, 8(3), 647–654. <https://doi.org/10.1007/s11947-014-1436-1>.
- Souza, M. P., Vaz, A. F. M., Silva, H. D., Cerqueira, M. A., Vicente, A. A., & Carneiro-da-Cunha, M. G. (2015b). Development and characterization of an active chitosan-based film containing quercetin.

- Food and Bioprocess Technology*, 8(11), 2183–2191. <https://doi.org/10.1007/s11947-015-1580-2>.
- Stenner, R., Matubayasi, N., & Shimizu, S. (2016). Gelation of carrageenan: effects of sugars and polyols. *Food Hydrocolloids*, 54, 284–292. <https://doi.org/10.1016/j.foodhyd.2015.10.007>.
- Toledo, C. E. P., Souza, M. A., Fraga, M. R., Ribeiro, L. C., Ferreira, A. P., & Vitral, R. W. F. (2012). Cellular viability and nitric oxide (NO) production by J774 macrophages in the presence of orthodontic archwires. *Journal Biomedical Science and Engineering*, 5(05), 255–262. <https://doi.org/10.4236/jbise.2012.55032>.
- Vera, P., Echegoyen, Y., Canellas, E., Nerín, C., Palomo, M., Madrid, Y., & Cámara, C. (2016). Nano selenium as antioxidant agent in a multilayer food packaging material. *Analytical and Bioanalytical Chemistry*, 408(24), 6659–6670. <https://doi.org/10.1007/s00216-016-9780-9>.
- Xia, Z., & Triffitt, J. T. (2006). A review on macrophage responses to biomaterials. *Biomedical Materials*, 1, 1–9.
- Yang, Z., Yang, H., & Yang, H. (2018). Effects of sucrose addition on the rheology and microstructure of κ -carrageenan gel. *Food Hydrocolloids*, 75, 164–173. <https://doi.org/10.1016/j.foodhyd.2017.08.032>.